JOURNAL OF SOLID STATE CHEMISTRY 35, 318–324 (1980)

The Structures of the $Na_3Ln(XO_4)_2$ Phases (Ln = Rare Earth, X = P, V, As)

M. VLASSE, C. PARENT, R. SALMON, G. LE FLEM, AND P. HAGENMULLER

Laboratoire de Chimie du Solide du CNRS, Université de Bordeaux I, 351 cours de la Libération, 33405 Talence, Cedex, France

Received January 16, 1980; in revised form February 25, 1980

Due to interest in new luminophors, a complete crystal chemical study of phases with the formulation $Na_3Ln(XO_4)_2$ (Ln = rare earth, X = P, V, As) has been undertaken. An overall description of these phases is given and relationships among various structural types are presented. The structural evolution is analyzed and discussed as a function of the rare-earth ion size and of the temperature.

In recent years interest in new luminophors has motivated considerable research into materials containing isolated rare-earth ions. Precise knowledge of the crystal structure is essential in studies of the luminescence properties of activator ions.

With this in mind, we have undertaken the study of compounds of formulation $Na_3Ln(XO_4)_2$ (Ln = rare earth and X = P, V, As) (*1–8*). The basic purpose of this work is to create ordering between Na^+ and Ln^{3+} within the lattice, due to the charge difference. This would lead to an increase in the distance between successive rare-earth ions and consequently to a decrease in self-concentration quenching.

For each Ln–X couple, there exist at least two allotropic varieties with related structures. Therefore, it is obviously necessary to present a systematic description of the $Na_3Ln(XO_4)_2$ phases and to discuss the relationships among various structural types as a function of the temperature and nature of the involved elements.

Table I gives crystallographic data for the nine structural types described in this study. The cell parameters of each of these phases are related to those of glaserite $K_3Na(SO_4)_2$ by elementary relationships. In addition, all the prototype structures of the low-temperature forms can be described using glaserite through the intermediate β-K_2SO_4 type for the larger Ln^{3+} ions and through the Na_2CrO_4 type (orthorhombic form) for the smaller Ln^{3+} ions.

In low-temperature forms, various types of Na–Ln ordering appear, depending on the rare-earth ion size. This ordering can be described by the sequence, along the [210] direction of the glaserite lattice, of rows containing either Na or Ln atoms. Most high-temperature phases adopt a disordered glaserite structure.

After the structures adopted by the different $Na_3Ln(XO_4)_2$ phases are briefly de-

0022-4596/80/150318-07$02.00/0

TABLE I

STRUCTURAL TYPES OF THE $Na_3Ln(XO_4)_2$ PHASES

	Structural type	Space group	Relationships between cell parameters of phases and those of glaserite hexagonal cell (a_h,c_h)	Z	Cationic ordering in B sublattice along [210] direction
I	$K_3Na(SO_4)_2$ glaserite (*10, 11*)	$P\bar{3}m1$	a_h; c_h	1	
II	β-K_2SO_4 (*12, 13*)	*Pnma*	$a_{orth} \simeq c_h$; $b_{orth} \simeq a_h$; $c_{orth} \simeq a_h 3^{1/2}$	4	
III	Na_2CrO_4 L.T. (*14*)	*Cmcm*	$a_{orth} \simeq a_h$; $b_{orth} \simeq a_h 3^{1/2}$; $c_{orth} \simeq c_h$	4	
IV	$Na_3La(VO_4)_2$ L.T. (*3*)	$Pbc2_1$	$a_{orth} \simeq a_h$; $b_{orth} \simeq 2c_h$; $c_{orth} \simeq 2a_h 3^{1/2}$	8	2–2
V	$Na_3Nd(VO_4)_2$ L.T. (*8*)	*Cc*	$a_{mon} \simeq 3a_h 3^{1/2}$; $b_{mon} \simeq a_h$; $c_{mon} \simeq 2c_h$	12	2–1
VI	$Na_3Nd(PO_4)_2$ L.T. (*5*)	$Pbc2_1$	$a_{orth} \simeq 3a_h$; $b_{orth} \simeq 2c_h$; $c_{orth} \simeq 2a_h 3^{1/2}$	24	2–2
VII	$Na_3Er(VO_4)_2$ L.T. (*4*)	$P2_1/n$	$a_{mon} \simeq a_h$; $b_{mon} \simeq a_h 3^{1/2}$; $c_{mon} \simeq c_h$	2	1–1
VIII	$Na_3Tm(PO_4)_2$ M.T. (*9*)	*Pnmm*, $Pnm2_1$	$a_{orth} \simeq 2a_h 3^{1/2}$; $b_{orth} \simeq c_h$; $c_{orth} \simeq 3a_h$	12	2–2
IX	$Na_3Yb(PO_4)_2$ H.T. (*7*)	$R\bar{3}c$	$a_{hex} \simeq a_h 3^{1/2}$; $c_{hex} \simeq 3c_h$;	9	

scribed, the structural evolution is analyzed and discussed.

A. Description of the Structures Adopted by the $Na_3Ln(XO_4)_2$ Phases

(*a*) $K_3Na(SO_4)_2$ (*Type I*)

Glaserite is the basic structure from which the eight remaining structures of Table I are derived. Its atomic arrangement, the hexagonal geometry of which defines the substructure observed in other $A_3B(XO_4)_2$ compounds, can actually be used as an ideal model in the establishment

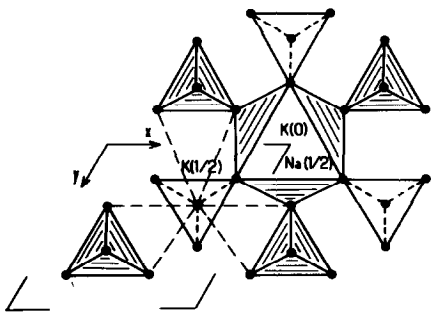

FIG. 1a. The glaserite structure projected down the threefold axis.

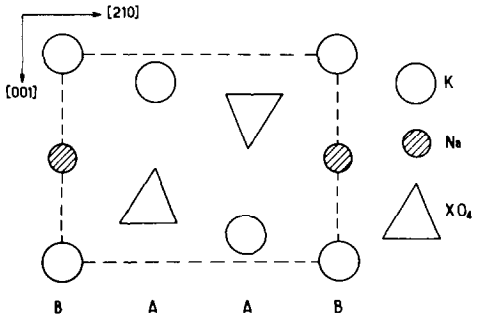

FIG. 1b. Rows of K and Na atoms (rows B) alternating with rows of [XO_4] tetrahedra and K atoms (rows A) in the glaserite lattice.

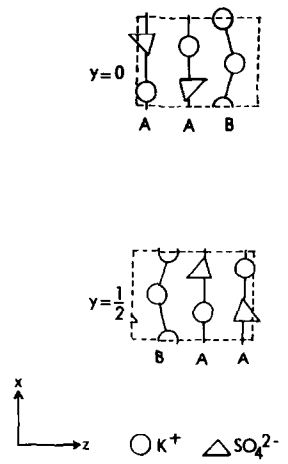

FIG. 2. A and B rows along the a axis of β-K_2SO_4.

of structural relationships among these compounds. The glaserite structure is characterized by two basic structural features:

(i) A central octahedron, with its threefold axis normal to the (001) plane linked at the corners to three up-pointing and three down-pointing tetrahedra (Fig. 1a).

(ii) In the (210) plane, rows of $[XO_4]$ tetrahedra and K atoms (rows A) alternating with rows of Na and K atoms (rows B), all running along the c axis (Fig. 1b). The coordination numbers are 10 and 12 for K and Na respectively.

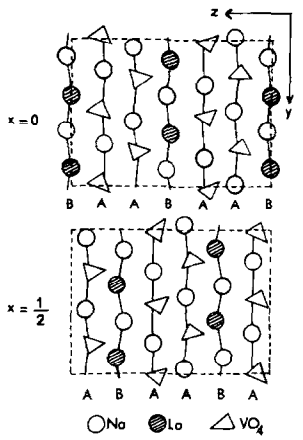

FIG. 3. Projection of the structure of L.T. $Na_3La(VO_4)_2$ on the (100) plane.

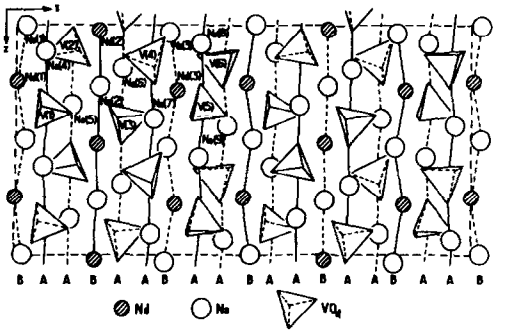

FIG. 4. Projection on the (010) plane of the L.T. $Na_3Nd(VO_4)_2$ structure: ——, y = ½; – – –, y = 0.

Both of these features are found in all other prototypes but in a somewhat distorted state. Glaserite, then, can be considered as the aristotype of the $Na_3Ln(XO_4)_2$ phases.

(b) β-K_2SO_4 (Type II), L.T. $Na_3La(VO_4)_2$ (Type IV) and L.T. $Na_3Nd(VO_4)_2$ (Type V)

The structure of β-K_2SO_4 is derived directly from the glaserite type with only a slight distortion: this can be seen by comparing the similar rows A ($[XO_4]$ and K) and B (K). The coordinations of potassium are 9 and 10 (Fig. 2). The structures of the low-temperature (L.T.) forms of $Na_3La(VO_4)_2$ and $Na_3Nd(VO_4)_2$ can be described as ordered superstructures of β-K_2SO_4, made up of rows either of alternating Na atoms and $[VO_4]$ tetrahedra (A) or of

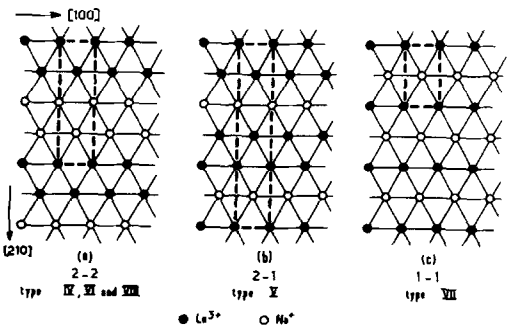

FIG. 5. Cationic ordering in the B sublattice along the [210] direction (cell is outlined by dotted lines).

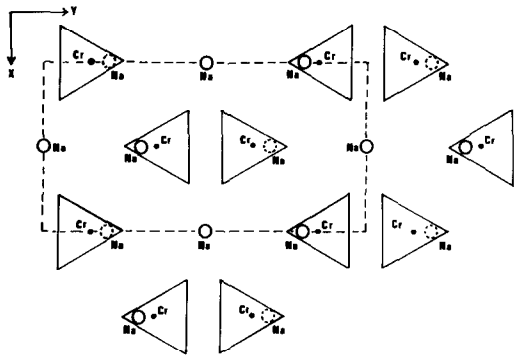

FIG. 6a. Projection of the Na_2CrO_4 structure on the (001) plane (orthorhombic form).

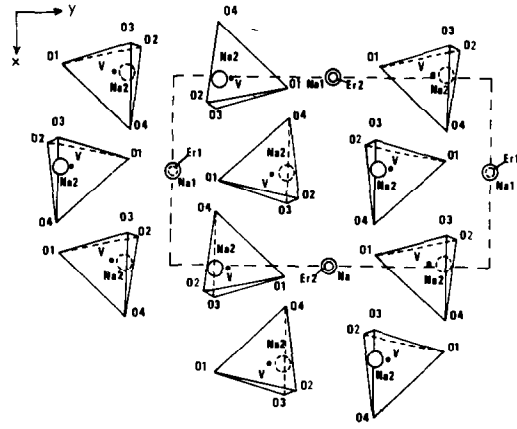

FIG. 7. Projection of the L.T. $Na_3Er(VO_4)_2$ structure on the (001) plane.

Na and rare-earth atoms (*B*) (Figs. 3 and 4).

In the *B* sublattice the Na–*Ln* ordering is of 1–1 (–Na–*Ln*—Na–*Ln*) type along the direction for the B rows but leads to different sequences along the [210] direction in certain planes of the glaserite lattice (Fig. 5). The sequence is 2–2 (two Na rows followed by two *Ln* rows) for type IV and 2–1 for type V. Within these structures, the rare-earth ions occupy respectively two and three crystallographic sites with eightfold coordination.

(*c*) *Na_2CrO_4 (Orthorhombic Form) (Type III) and L.T. $Na_3Er(VO_4)_2$ (Type VII)*

The structure of Na_2CrO_4 (orthorhombic form) is again a very slightly distorted version of the glaserite lattice (Fig. 6). The main difference is a small rotation of the central octahedron and its associated tetrahedra about the threefold axis. Similar A and B rows are found; however, all sodium atoms are in octahedral sites.

In L.T. $Na_3Er(VO_4)_2$ (type VII) (Fig. 7) the only difference is a 1–1 ordering along the direction of the *B* rows and also along the [210] direction of the glaserite structure (Fig. 5). The erbium atom occupies a slightly distorted octahedral site.

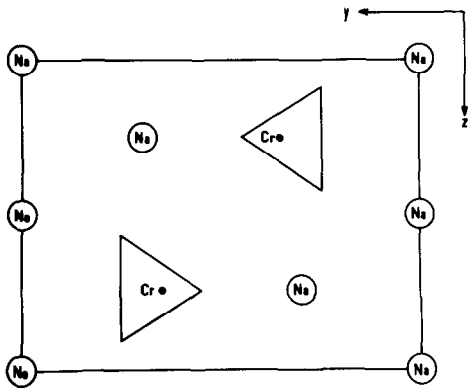

FIG. 6b. A and B rows running along the c axis of Na_2CrO_4 (orthorhombic form).

(*d*) *L.T. $Na_3Nd(PO_4)_2$ (Type VI) and M.T. $Na_3Tm(PO_4)_2$ (Type VIII)*

These structural types can be considered as intermediate between β-K_2SO_4 and

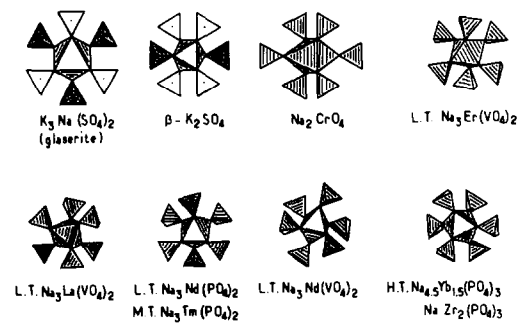

FIG. 8. Basic building blocks found in the $Na_3Ln(XO_4)_2$ structures.

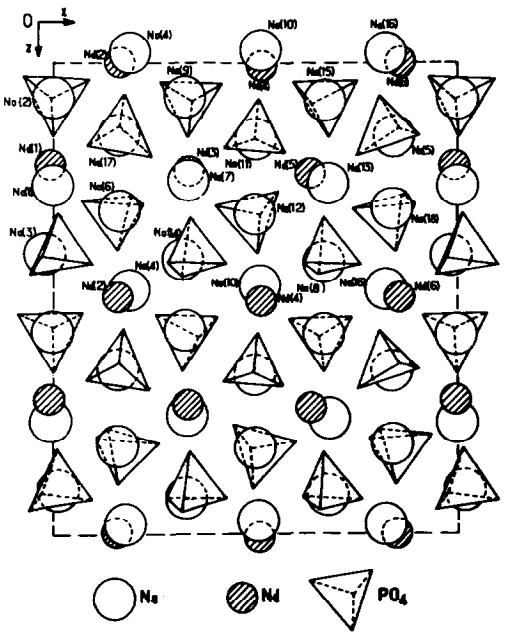

FIG. 9. Projection of the basic slab of the $Na_3Nd(PO_4)_2$ structure on the (010) plane.

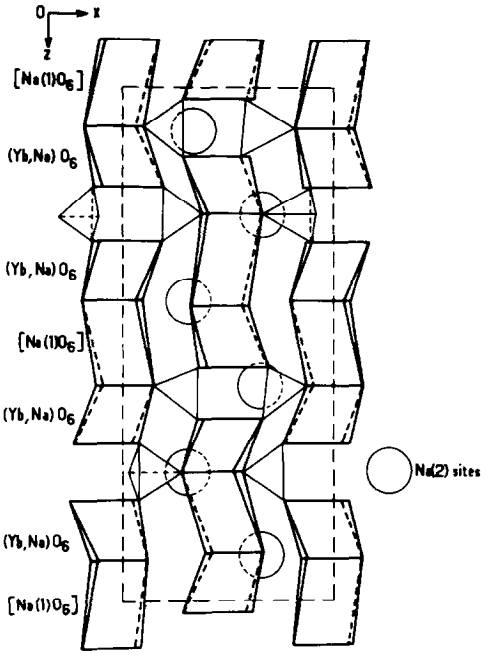

FIG. 10b. Projection of $Na_{4.50}Yb_{1.50}(PO_4)_3$ along the [120] direction.

Na_2CrO_4 (orthorhombic form). The six $[XO_4]$ tetrahedra surrounding the central octahedron are able to rotate, accommodating various coordinations of the rare-earth ion (Fig. 8). In $Na_3Nd(PO_4)_2$ (Fig. 9) this marked rotation leads to six different sites for neodymium with various coordinations (6, 7, and 8). The cationic ordering is 2–2 along the [210] direction of glaserite (Fig. 5).

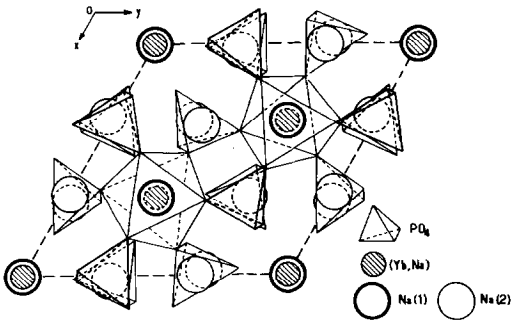

FIG. 10a. Projection of one-third of the unit cell of H.T. $Na_{4.50}Yb_{1.50}(PO)_4)_3$ along the c axis.

Although the structure of the medium-temperature (M.T.) form of $Na_3Tm(PO_4)_2$ has not been determined by single-crystal diffraction analysis, it can be claimed without any doubt to be very comparable to that of $Na_3Nd(PO_4)_2$. This is corroborated by practically identical powder diffraction patterns and cell parameters, except that $b_{VIII} \simeq \frac{1}{2}b_{VII}$. Therefore, one can expect the same cationic distribution and the same coordination polyhedra for the Na and *Ln* atoms.

(*e*) *H.T. $Na_3Yb(PO_4)_2$ (Type IV)*

This particular structure derives directly from the $NaZr_2(PO_4)_3$ type (*15*). A partial projection is given in Fig. 10a. It can be described as a three-dimensional framework made up of central [(Na, Yb)O_6] and [Na(1)O_6] octahedra and their six associated [PO_4] tetrahedra. The rigid three-dimensional skeleton forms a stable lattice, the Na(2) atoms occupying large holes with 10-fold coordination.

The [Na(1)O_6] octahedron shares opposite faces with the [(Yb, Na)O_6] octahedra, giving rise to [(Yb, Na)O_6][Na(1)O_6] [(Yb, Na)O_6] groups oriented in a direction parallel to the c axis (Fig. 10b). By contrast to the types discussed above, ordering between Na^+ and Ln^{3+} along this direction is no longer strictly 1–1.

The three-dimensional skeleton assumes the cohesion of the lattice, while the Na(2) interstitial sites can be empty or partially or fully occupied. It explains the ability of phases of this type to be nonstoichiometric and accordingly their more general formulation: $Na_{3(1+x)}Ln_{(2-x)}(XO_4)_3$ ($0 \leq x \leq 0.50$).

B. Relationships among the Various Structural Types

In all these structures, a glaserite-type building block is found. The capacity of the glaserite structure to form all the related structures is due to the ability of the [XO_4] groups to rotate in order to accommodate different coordinations of the rare-earth ions (Fig. 8).

For the larger rare-earth ions, the coordination is 8 (type IV); for the smaller, it is only 6 (type VII). In structures involving an intermediate Ln^{3+} size, one observes for the same phase various coordinations (6, 7, and 8 in the case of $Na_3Nd(PO_4)_2$) and consequently a greater number of sites for the rare-earth ion (three in $Na_3Nd(VO_4)_2$, six in $Na_3Nd(PO_4)_2$).

C. Na^+–Ln^{3+} Ordering as a Function of the Rare-Earth Ion Size

In the low-temperature forms, various types of Na^+–Ln^{3+} ordering appear depending on the size of the rare-earth ion. Variation of this ordering can be described by representing in the *B* sublattice the sequence along the [210] direction of the glaserite lattice of cationic rows (Fig. 5).

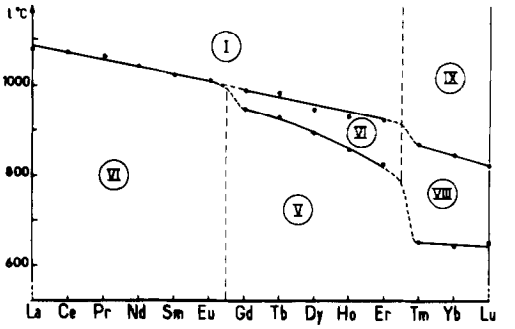

FIG. 11a. Thermal behavior of the $Na_3Ln(PO_4)_2$ phases.

For structural types IV, VI, and VIII, the sequence is 2–2. In the planes perpendicular to the A and B rows each Na^+ is surrounded by four Na^+ and two Ln^{3+} ions, each Ln^{3+} by four Ln^{3+} and two Na^+ ions (Fig. 5a). For structural type VII, the sequence is 1–1: each Na^+ is surrounded by four Ln^{3+} and two Na^+ and vice versa (Fig. 5c).

Within type V one can observe an intermediate distribution: along the [210] direction, in the *B* sublattice, the cationic ordering is 2–1. Two types of rare-earth–sodium planes alternate. In the first, each Na^+ ion is surrounded by four Ln^{3+} and two Na^+ ions. In the second, the opposite is observed (Fig. 5b).

When the rare-earth ion becomes larger, ordering between Na^+ and Ln^{3+} decreases.

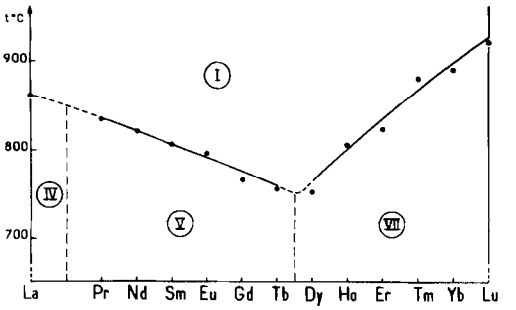

FIG. 11b. Thermal behavior of the $Na_3Ln(VO_4)_2$ phases.

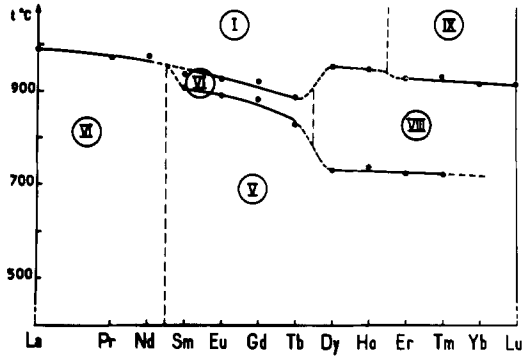

FIG. 11c. Thermal behavior of the $Na_3Ln(AsO_4)_2$ phases.

The influence of the nature of the (XO_4) group on the structure is more difficult to understand.

D. Structural Evolution of $Na_3Ln(XO_4)_2$ Phases as a Function of Temperature

The distribution of the various $Na_3Ln(PO_4)_2$, $Na_3Ln(VO_4)_2$, and $Na_3Ln(AsO_4)_2$ phases as a function of temperature is shown in Fig. 11. The structural and thermal behaviors of the phosphates and arsenates are very similar, with only slight changes in the middle of the diagram. However, the vanadates show much simpler thermal and structural behavior. For every compound the transitions are reversible, except for V → VIII.

An increase in temperature leads to an increase in disordering. For most compounds the higher-temperature form has a glaserite-type structure, which is the result of a real order–disorder transition in the *B* sublattice. For the other materials the appearance of a $NaZr_2(PO_4)_3$-type phase (type IX) results from a rearrangement due to the ability of the smaller rare-earth ions to accommodate an octahedral site.

Finally, certain vanadate phases (*Ln* = Y, Dy, Ho, Er, Tm, Yb, Lu) adopt the metastable Na_2CrO_4-type (orthorhombic form) structure (type III) by very fast quenching from high temperature. This structure, intermediate between $K_3Na(SO_4)_2$ (type I) and $Na_3Er(VO_4)_2$ (type VII) readily converts to the stable type VII by annealing at low temperature.

A recent study shows that the effect of pressure on the various phases investigated is similar to an increase in size of the rare-earth ion, both phenomena being a consequence of higher cationic repulsion (*16*).

References

1. R. SALMON, C. PARENT, A. BERRADA, R. BROCHU, A. DAOUDI, M. VLASSE, AND G. LE FLEM, *C.R. Acad. Sci. Paris* **280**, 805 (1975).
2. R. SALMON, C. PARENT, A. DAOUDI, AND G. LE FLEM, *Rev. Chim. Miner.* **12**, 448 (1975).
3. M. VLASSE, R. SALMON, AND C. PARENT, *Inorg. Chem.* **15**, 1440 (1976).
4. R. SALMON, C. PARENT, G. LE FLEM, AND M. VLASSE, *Acta Crystallogr. Sect. B* **32**, 2799 (1976).
5. R. SALMON, C. PARENT, M. VLASSE, AND G. LE FLEM, *Mater. Res. Bull.* **13**, 439 (1978).
6. C. PARENT, R. SALMON, AND G. LE FLEM, *C.R. Acad. Sci. Paris* **286**, 365 (1978).
7. R. SALMON, C. PARENT, M. VLASSE, AND G. LE FLEM, *Mater. Res. Bull.* **14**, 85 (1979).
8. C. PARENT, J. FAVA, R. SALMON, M. VLASSE, G. LE FLEM, P. HAGENMULLER, E. ANTIC-FIDANCEV, M. LEMAITRE-BLAISE, AND P. CARO, *Nouv. J. Chimie* **3**, 523 (1979).
9. S. K. APINITIS AND Y. IA SEDMALIS, *Izv. Akad. Nauk Latv. SSR* **3**, 373 (1978).
10. B. GOSSNER, *Neues Jahrb. Mineral.* **57**, 89 (1928).
11. H. F. FISCHMEISTER, *Monatsh. Chem.* **93**, 420 (1962).
12. M. T. ROBINSON, *J. Phys. Chem.* **62**, 925 (1952).
13. G. GAULTIER AND G. PANNETIER, *Bull. Soc. Chim. Fr.* **1**, 105 (1968).
14. A. NIGGLI, *Acta Crystallogr.* **7**, 776 (1954).
15. L. O. HAGMAN AND P. KIERKEGAARD, *Acta Chem. Scand.* **22**, 1822 (1968).
16. C. PARENT, G. DEMAZEAU, R. SALMON, AND G. LE FLEM, *Rev. Chim. Miner.*, **16**, 548 (1979).